Title	High-energy gamma-ray emission from anomalous X-ray pulsars
Author(s)	Cheng, KS; Zhang, L
Citation	Astrophysical Journal Letters, 2001, v. 562 n. 2 PART II, p. 918-924
Issued Date	2001
URL	http://hdl.handle.net/10722/43336
Rights	Creative Commons: Attribution 3.0 Hong Kong License

THE ASTROPHYSICAL JOURNAL, 562:918–924, 2001 December 1

HIGH-ENERGY GAMMA-RAY EMISSION FROM ANOMALOUS X-RAY PULSARS

K. S. CHENG[1] AND L. ZHANG[1,2]

Received 2001 April 18; accepted 2001 July 31

ABSTRACT

We study the high-energy gamma-ray radiation from the outer magnetospheres of the anomalous X-ray pulsars. For pulsars with superstrong magnetic fields ($B > 10^{14}$ G), the magnetic field in the region far away from the neutron star surface drops below the quantum critical value, and high-energy gamma-ray emission can be emitted. The electrons/positrons produced by collisions between high-energy photons from the outer gap and the soft X-rays resulting from the stellar surface are accelerated inside the outer gap and emit the high-energy gamma rays through curvature radiation. The gamma-ray spectrum and luminosity in this model can be estimated once the pulsar parameters such as period, surface magnetic field, and surface temperature are given. We apply this model to some anomalous X-ray pulsars such as 4U 0142+615, 1E 1048.1−5937, RX J170849−4009, 1E 1841−045, and 1E 2259+586 and suggest that their gamma-ray fluxes could be detected by the *Gamma-Ray Large-Area Space Telescope*.

Subject headings: gamma rays: theory — pulsars: general — stars: neutron

1. INTRODUCTION

The anomalous X-ray pulsars (AXPs) consist of a small group of neutron stars characterized by periods of several seconds and by the absence of massive companion stars (Mereghetti & Stella 1995; van Paradijs, Taam, & van den Heuvel 1995). They have been detected through their persistent X-ray pulsations, and several of these AXPs are associated with supernova remnants, indicating that they are young objects. Because of their long periods, the rotational energy loss of the AXPs is too low to account for their observed X-ray luminosities. Briefly, AXPs share several typical properties: (1) a narrow interval of pulse periods (6–12 s); (2) very soft X-ray spectrum characterized by the sum of a steep power law with photon index of $\sim$3–4 and an additional blackbody-like component with a temperature of $\sim$0.4–0.6 keV; (3) relatively low and steady X-ray luminosity ($\sim 10^{35}$–10^{36} ergs s^{-1}); (4) relatively stable spin period evolution with long-term spin-down trend [the relatively stable rate is (2–100) $\times 10^{-5}$ s yr^{-1}]; and (5) an absence of massive companion stars (see Mereghetti 1999 for a review). Now there are two kinds of models to explain the observed properties of AXPs. One is that X-ray emission is powered by accretion either in a low-mass X-ray binary (Mereghetti & Stella 1995) or through a fossil disk (van Paradijs et al. 1995). The other is that AXPs are assumed to be either ultramagnetized neutron stars (Thompson & Duncan 1996) or remnants of Thorne-Zytkow objects (van Paradijs et al. 1995).

Growing evidence indicates that soft gamma-ray repeaters (SGRs) and AXPs are magnetars (e.g., Kouveliotou et al. 1998, 1999; Hurley et al. 1999). The AXPs and those SGRs with observed rotation periods all have spin periods $P \sim 6$–12 s; measured period derivatives show spin-down in the range $|\dot{\Omega}| \sim 10^{-12}$–$10^{-13}$ rad s^{-2}; and their persistent X-ray luminosities ($L_X \sim 3 \times 10^{34}$–$10^{36}$ ergs s^{-1}) and their soft X-ray spectra are similar. These sources have all been proposed to be magnetars, neutron stars with dipole magnetic fields of the order of 10^{14}–10^{15} G. The X-ray emission could be powered by magnetic field decay (Thompson & Duncan 1996; Heyl & Kulkarni 1998). Such strong magnetic fields are above the quantum critical field, $B_c = m_e^2 c^3/e\hbar \approx 4.4 \times 10^{13}$ G, for which a photon at the electron cyclotron energy can create electron positron pairs. A simple way to check for a magnetar is to look for the gamma-ray spectrum. Because of the strong field of a magnetar, the gamma-ray emission rooted at the polar caps will be quenched. However, far away from the pulsar surface, i.e., in the outer gaps, the gamma rays will be emitted from these regions because the local magnetic field will drop below the quantum critical value.

In the outer magnetospheric gap model (Cheng, Ho, & Ruderman 1986; Ruderman & Cheng 1988; Cheng & Ding 1994; Zhang & Cheng 1997), high-energy gamma-ray emission is produced for pulsars with a suitable period–magnetic field combination, such that the voltage is high enough to create pairs to sustain the accelerator (gap). The gamma-ray flux and spectrum may also depend on neutron star surface temperature if the outer gap pair production mechanism is dominated by thermal photons from the stellar surface (Zhang & Cheng 1997). Here we apply this model to predict the gamma-ray emission from the magnetar magnetosphere. In § 2, we describe the gamma-ray emission model. We apply it to individual AXPs in § 3, and a discussion is presented in § 4.

2. THE GAMMA-RAY EMISSION MODEL

Zhang & Cheng (1997) have considered a self-sustained gap-closing mechanism in which the size of the gap is limited by the $e^{\pm}$ pairs produced by collisions between high-energy photons from the gap and the soft X-rays resulting from the surface heating by the backflow primary

[1] Department of Physics, University of Hong Kong, Hong Kong, China.
[2] Department of Physics, Yunnan University, Kunming, China; hrspksc@khucc.hku.hk, lzhang@bohr.physics.hku.hk.

$e^{\pm}$ pairs. In this model, the Lorentz factor, γ_e, of the accelerated $e^{\pm}$ pairs in the outer gap can be estimated approximately by $eE_{\parallel} c = P_{\rm cur}$, where $E_{\parallel}$ is the electric field along the magnetic field and $P_{\rm cur}$ is the curvature radiation power. Thus, the characteristic energy of the gamma-ray photons in the outer gap is $E_{\gamma}(f) = (3/2)\hbar\gamma_e^3(c/s)$, which can be approximated as (Zhang & Cheng 1997)

$$E_{\gamma} \approx 2 \times 10^8 f^{3/2} B_{12}^{3/4} P^{-7/4} R_6^{9/4} \ \text{eV} , \qquad (1)$$

where P is the pulsar period in units of seconds, B_{12} is the dipolar magnetic field in units of 10^{12} G, and R is the radius of the neutron star in units of 10^6 cm. The return particle flux can be approximated as $\dot{N}_e = f\dot{N}_{\rm GJ}$, where f is the fractional volume of the outer magnetosphere occupied by the outer gap and $\dot{N}_{\rm GJ}$ is the Goldreich and Julian particle flux. The size of the outer gap, f, is limited by the pair production between the thermal X-rays with energy $E_{\rm X}(f)$ from the stellar surface and the gamma-ray photons with energy $E_{\gamma}(f)$ emitted by the primary electrons/positrons accelerated in the outer gap. There are two possible kinds of the origins of the soft X-ray photons. First, one-half of the primary $e^{\pm}$ pairs in the outer gap will move toward the star and lose their energy via the curvature radiation. Although most of the energy of the primary particles will be lost on the way to the star via curvature radiation, about $10.6P^{1/3}$ ergs particle^{-1} will still remain and will finally be deposited on the stellar surface. This energy will be emitted via X-rays from the stellar surface (Halpern & Ruderman 1993). The characteristic energy of X-rays is given by $E_{\rm X}^h \approx 3kT \approx 1.2 \times 10^3 P^{-1/6} B_{12}^{1/4}$ eV. The keV X-rays from a hot polar cap will be reflected back to the stellar surface because of the cyclotron resonance scattering if there is a large density of magnetic-produced $e^{\pm}$ pairs near the neutron star surface (Halpern & Ruderman 1993; Wang et al. 1998) and eventually reemitted as softer thermal X-rays with characteristic energy $E_{\rm X}^s \approx 0.1 f^{1/4} P^{-1/4} E_{\rm X}^h$. This means that the soft X-ray energy $E_{\rm X}(f)$ is also a function of the gap size. Using $E_{\rm X}(f)E_{\gamma}(f) \sim (mc^2)^2$, the fractional size of the outer gap, f, can be expressed in terms of P and B_{12}. Although the original X-ray photon density is low, every pair resulting from X-ray and curvature photon interactions can emit $\sim 10^5$ photons in the outer gap. Such a large multiplicity can produce sufficient numbers of $e^{\pm}$ pairs so as to sustain the outer gap. We have applied such a model to explain the gamma-ray emission from gamma-ray pulsars (see Zhang & Cheng 1997, 1998; Cheng & Zhang 1998). Second, if the thermal X-rays produced by the cooling mechanism of the neutron star are dominated, the X-ray energy does not depend on f. In this case, according to Zhang & Cheng (1997), the size of the outer gap is $f \approx 4.5 P^{7/6} B_{12}^{-1/2} T_{s6}^{-2/3} R_6^{-3/2}$ with the surface temperature of the star $T_{s6} = T_s/10^6$ K.

For the magnetar, it is believed that the thermal emission from the stellar surface is powered by the decay of the strong magnetic field (see, e.g., Thompson & Duncan 1993, 1996) or by neutron star cooling (Heyl & Hernquist 1997) and contributes significantly to the soft X-ray flux. Here we assume that the soft photons to sustain the outer gap are provided by these soft X-rays. In fact, f is larger than unity without these soft X-rays (cf. eq. [22] of Zhang & Cheng 1997). Generally, the temperature distribution of the thermal emission from the surface of the magnetar is anisotropic (for detailed calculations see Heyl & Hernquist 1997; Özel 2001; Özel, Psaltis, & Kaspi 2001). Following Zhang & Cheng (1997), the size of the outer gap can be expressed as

$$f \approx 0.68 \left(\frac{P}{6\ \text{s}}\right)^{7/6} \left(\frac{B}{10^{14}\ \text{G}}\right)^{-1/2} \times \left[\frac{T_s(\theta)}{5 \times 10^6\ \text{K}}\right]^{-2/3} \left(\frac{R}{15\ \text{km}}\right)^{-3/2} , \qquad (2)$$

where $T_s(\theta)$ is the surface temperature of the magnetar, which is a function of the polar angle (θ) with respect to the magnetic axis. For example, the temperature distribution on the stellar surface for a cooling neutron star with a strong magnetic dipole is $T_s(\theta) = T_p g^{1/4}(\theta)$, where T_p is the temperature of the magnetic pole and $g(\theta) = \cos^2\theta/(3\cos^2\theta + 1)^{0.8}$ (Heyl & Hernquist 1997). Putting this expression into equation (2), we have $f \propto g^{1/6}(\theta)$. When θ changes from 0° to 60°, we have $f(\theta = 0°)/f(\theta = 60°) \approx 1.1$. It seems that the fractional size of the outer gap has a weak dependence on the polar angle (θ) at a certain angular range (say 0°–60°). Therefore, for simplicity, we ignore the dependence of the temperature on the polar angle and estimate it from the quiescent X-ray luminosity $L_{\rm X}$ of magnetars by $T_{s6} \approx 4.8(L_{\rm X}/10^{35})^{1/4} R_6^{-1/2}$. For the typical parameters of the magnetar, $P = 8$ s, $B = 5 \times 10^{14}$ G, $T_s = 5 \times 10^6$ K, and $R = 15$ km, we have $f \approx 0.43$, which means that the outer gap is "thick." As pointed out by Zhang & Cheng (1997), f could not be greater than unity; otherwise the outer gap does not exist. It should be pointed out that the fractional size of the outer gap for an AXP decreases with increasing surface temperature T_s because $f \propto T_s^{-2/3}$ in our model. We have estimated the fractional sizes of the outer gap for various AXPs using equation (2); these are listed in Table 1. Because the period derivatives of two AXPs (RX J1838.4−0301 and AX J1845.0−0300) have not been detected, we cannot estimate their fractional sizes of the outer gap. Furthermore, the fractional size of the outer gap for RX J0720.4−3125 is greater than unity, which means that its outer gap does not exist, so we do not consider it further in this paper.

For the thick outer gap, gamma rays are produced inside the thick outer gap by curvature radiation from the primary $e^{\pm}$ pairs along the curved magnetic field lines. Zhang & Cheng (1997) have shown that the primary $e^{\pm}$ pairs have an approximate power-law distribution inside the outer gap because the energy and density of the primary $e^{\pm}$ pairs depend on local values of the magnetic field, electric field, and radius of curvature. In steady state, the energy distribution of the accelerated particles in the outer gap is

$$\frac{dN}{dE_e} \propto \left(\frac{\gamma}{\gamma_0}\right)^{-16/3} , \qquad (3)$$

where E_e is the energy of the accelerated particle. It should be noted that the Lorentz factor in equation (3) is the function of x given by (Zhang & Cheng 1997)

$$\gamma(x) \approx \gamma_0 x^{-3/4} \quad \text{for} \quad x_{\rm min} \le x \le x_{\rm max} , \qquad (4)$$

where $\gamma_0 \approx 2.8 \times 10^7 f^{1/2} B_{12}^{1/4} P^{-1/4} (R/10\ \text{km})^{3/4}$, $x = s/R_L$, s is the local radius of curvature, and R_L is the radius of the light cylinder; $x_{\rm min}$ and $x_{\rm max}$ are minimum and maximum curvature radii in units of the radius of the light cylinder. Using $(dN/dE_e)dE_e = (dN/dx)dx$, the curvature radiation spectrum produced by the primary particles can be

TABLE 1

ANOMALOUS X-RAY PULSARS

Pulsar	Other Name	P (s)	$\dot{P}_{-11}$[a] ($\times 10^{-11}$ s s^{-1})	B_{14}[b] ($\times 10^{14}$ G)	T_{s6}[c] ($\times 10^{6}$ K)	$d_{\rm kpc}$[d] (kpc)	L_X[e] ($\times 10^{35}$ ergs s^{-1})	f	F_γ[f] ($\times 10^{-8}$ cm^2 s^{-1})
4U 0142+615	AXP 0142+615	8.69	~0.2	2.6	4.5	>2.7	$\sim 18 d_3^2$	0.70	$3.1 d_3^{-2}$
RX J0720.4−3125	AXP 0720−3125	8.39	0.26	~1	0.09	0.3	0.002	3.1	...
1E 1048−5937	AXP 1048−5937	6.44	1.5–4	>6.3	7.4	2.5–2.8	$\sim 0.3 d_{2.5}^2$	0.23	$4.8 d_{2.5}^{-2}$
RX J170849−4009.....	AXP 1709−40	11.0	2	9.5	4.6	3.0–5.0	$\sim 0.9 d_3^2$	0.47	$5.1 d_3^{-2}$
RX J1834.4−0301	AXP 1834−03	5.45	...	...	...	5.2	0.6	...	...
1E 1841−045.....	AXP 1841−045	11.76	4.7	14	6.4	6.0–7.5	$\sim 2.6 d_6^2$	0.39	$1.3 d_6^{-2}$
AX J1845.0−0300	...	6.97	...	...	7.4	8.5	0.91	...	...
1E 2259+58.6	AXP 2259+58.6	6.98	~0.05	1.2	4.8	3.6–5.5	$\sim 0.6 d_{3.6}^2$	0.76	$1.5 d_{3.6}^{-2}$

[a] Period derivative.
[b] Surface magnetic field.
[c] Surface temperature of the pulsar.
[d] Distance to the pulsar.
[e] Observed X-ray luminosity, where $d_3 = d/(3\ \mathrm{kpc})$.
[f] Expected gamma-ray flux with energy greater than 100 MeV using equation (12), where $d_3 = d/(3\ \mathrm{kpc})$.

expressed as

$$\frac{d^2N_\gamma}{dE_\gamma\, dt} \approx \frac{\dot{N}_0}{E_\gamma} \int_{x_{\rm min}}^{x_{\rm max}} x^{1/2} F(y)\, dx\ , \tag{5}$$

where $\dot{N}_0 = \sqrt{3} e^2 \gamma_0 N_0 / h R_L$ and $N_0 \approx 1.4 \times 10^{30} f (B_{12}/P)(R/10\ \mathrm{km})^3$; $F(y) = \int_y^\infty K_{5/3}(z) dz$, where $K_{5/3}$ is the modified Bessel function of order 5/3, and $y = E_\gamma / E_c$. The characteristic energy of the radiated photons is given by equation (1). The differential flux at the Earth is given by

$$F(E_\gamma) = \frac{1}{\Delta\Omega d^2} \frac{d^2N_\gamma}{dE_\gamma\, dt}\ , \tag{6}$$

where $\Delta\Omega$ is the solid angle of gamma-ray beaming and d is the distance to the pulsar. In this model, the three parameters, $\Delta\Omega$, $x_{\rm min}$, and $x_{\rm max}$, depend on the detailed structure of the outer gap and the inclination angle of the pulsar. $x_{\rm min}$, is estimated to be the intersection of the last open field line and null charge surface. If the inclination angle is greater than 45°, we have

$$x_{\rm min} \approx \frac{2}{3 \tan \alpha}\ , \tag{7}$$

where α is the magnetic inclination angle. Furthermore, the integral flux with energy greater than a certain value E_i is given by

$$F(\geq E_i) = \frac{1}{\Delta\Omega d^2} \int_{E_i}^{E_{\rm max}} \frac{d^2N_\gamma}{dE_\gamma\, dt}\ , \tag{8}$$

where $E_{\rm max}$ is the maximum energy of gamma rays.

According to Zhang & Cheng (1997), the gamma-ray luminosity provided by the outer gap is

$$L_\gamma \approx 4.0 \times 10^{32} \left(\frac{f}{0.5}\right)^3 \left(\frac{B}{10^{14}\ \mathrm{G}}\right)^2 \times \left(\frac{P}{6\ \mathrm{s}}\right)^{-4} \left(\frac{R}{15\ \mathrm{km}}\right)^6 \mathrm{ergs\ s^{-1}}\ . \tag{9}$$

It can be seen that the gamma-ray luminosity is less than the observed X-ray luminosity by 2 or 3 orders. For example, the observed X-ray luminosity of 4U 0142+615 is $\sim 4.5 \times 10^{35}$ ergs s^{-1}, but the expected gamma-ray luminosity is $\sim 1.4 \times 10^{33}$ ergs s^{-1}, $L_\gamma / L_X \sim 3 \times 10^{-3}$.

As examples, we calculate the expected gamma-ray fluxes using the typical parameters of the AXPs. In our calculations, we assume that $x_{\rm max} = 2$, and $x_{\rm min}$ is estimated by using equation (7). The expected gamma-ray spectrum for a given pulsar is normalized so that the value of the integral

$$\Delta\Omega d^2 \int_{E_{\rm min}}^{E_{\rm max}} E_\gamma F(E_\gamma) dE_\gamma \tag{10}$$

equals the value given by equation (9), where $E_{\rm min}$ and $E_{\rm max}$ are the minimum and maximum energies of the gamma rays; here we set $E_{\rm min} = 1$ MeV and $E_{\rm max} = 100$ GeV. In Figure 1, we show the expected gamma-ray fluxes of a pulsar with typical parameters of $P = 10$ s, $B_{14} = 10$, and $T_s = 5 \times 10^6$ K for different magnetic inclination angles. It can be seen that the gamma-ray spectrum will extend to a higher energy region as the magnetic inclination angle

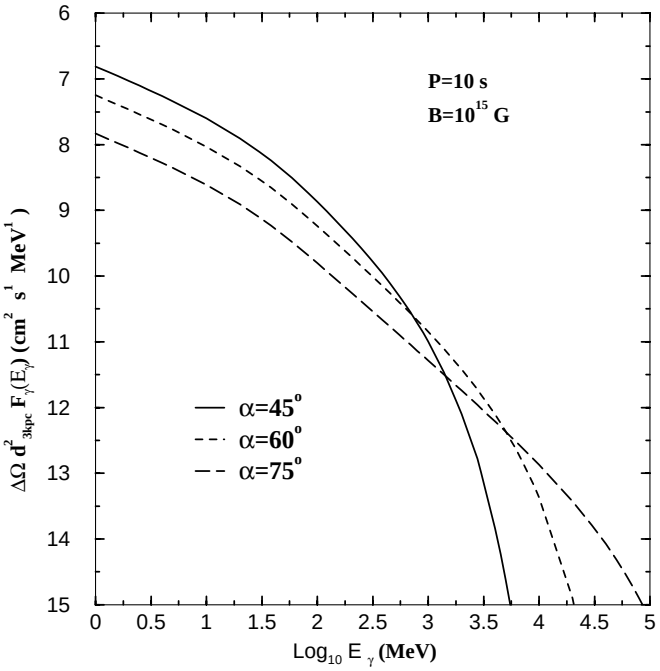

FIG. 1.—Expected gamma-ray spectrum of an AXP. The pulsar's parameters are as follows: $P = 10$ s, $B_{14} = 10$, and $T_s = 5 \times 10^6$ K. The solid, dashed, and long-dashed curves represent the expected gamma-ray fluxes for the magnetic inclination angles of 45°, 60°, and 75°, respectively.

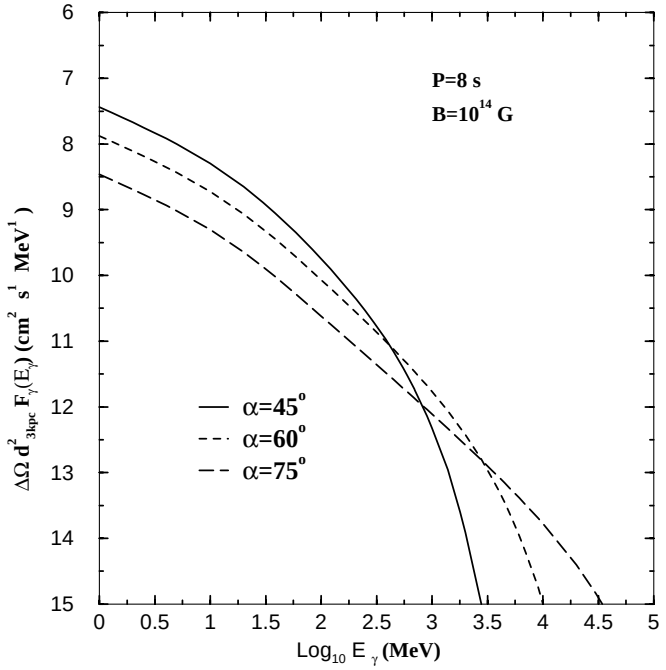

FIG. 2.—Same as Fig. 1 but for a pulsar with the following parameters: $P = 8$ s, $B_{14} = 1$, and $T_s = 5 \times 10^6$ K.

increases. In this case, the fractional size is $f \approx 0.57$ and the total gamma-ray luminosity is $L_\gamma \approx 7.7 \times 10^{33}$ ergs s^{-1}. In Figure 2, the expected gamma-ray fluxes of a pulsar with typical parameters of $P = 8$ s, $B_{14} = 1$, and $T_s = 5 \times 10^6$ K for different magnetic inclination angles are shown, where $f \approx 0.95$ and $L_\gamma \approx 8.7 \times 10^{32}$ ergs s^{-1}. In Figure 3, the expected gamma-ray fluxes of a pulsar with $P = 6$ s, $B_{14} = 5$, and $T_s = 5 \times 10^6$ K for different magnetic inclination angles are shown, where $f \approx 0.3$ and $L_\gamma \approx 2.2 \times 10^{33}$ ergs s^{-1}.

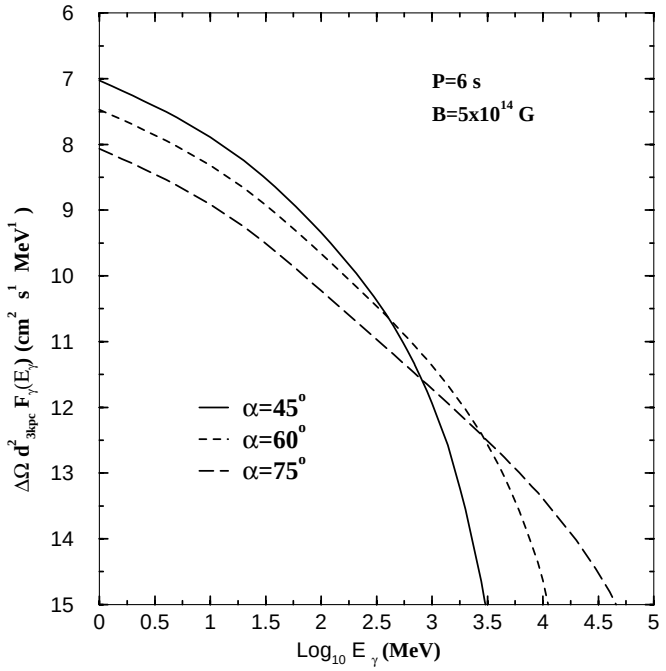

FIG. 3.—Same as Fig. 1 but for a pulsar with the following parameters: $P = 6$ s, $B_{14} = 5$, and $T_s = 5 \times 10^6$ K.

3. APPLICATIONS TO ANOMALOUS X-RAY PULSARS

Eight AXPs have been detected, but the period derivatives of two of them are not determined yet (e.g., see Liu, van Paradijs, & van den Heuvel 2001). According to Marsden et al. (2001), five AXPs are associated with supernova remnants (SNRs). Because of the distance uncertainty, the expected gamma-ray flux will be uncertain. Before considering an individual AXP, we give an approximate estimate of the gamma-ray flux with energy greater than 100 MeV in our model.

We can approximately estimate the gamma-ray integrated flux of each magnetar as follows. Because the average characteristic energy of the radiated photons can be approximated as

$$\langle E_c \rangle \approx 3.9 \times 10^{-4} \left(\frac{f}{0.5}\right)^{3/2} \left(\frac{B}{10^{14}\ \mathrm{G}}\right)^{3/4} \times \left(\frac{P}{6\ \mathrm{s}}\right)^{-7/4} \left(\frac{R}{15\ \mathrm{km}}\right)^{9/4} \mathrm{ergs}\ , \quad (11)$$

the integrated flux for each magnetar is approximated as $F_\gamma^{\mathrm{th}} \approx (L_\gamma / \Delta\Omega d^2 \langle E_c \rangle)$. Because L_γ represents the total gamma-ray luminosity for the entire energy range, the integrated flux with energy greater than 100 MeV can be approximated as

$$F_\gamma^{\mathrm{th}}(\geq 100\ \mathrm{MeV}) \approx \frac{1.3 \times 10^{-8}}{d_{3\ \mathrm{kpc}}^2\, \Delta\Omega} \left(\frac{f}{0.5}\right)^{3/2} \left(\frac{B}{10^{14}\ \mathrm{G}}\right)^{5/4} \times \left(\frac{P}{6\ \mathrm{s}}\right)^{-9/4} \left(\frac{R}{15\ \mathrm{km}}\right)^{15/4} \mathrm{cm}^{-2}\ \mathrm{s}^{-1}\ , \quad (12)$$

where $d_{3\ \mathrm{kpc}}$ is the distance in units of 3 kpc and $\Delta\Omega$ is in steradians. In equation (12), F_γ^{th} involves the solid angle $\Delta\Omega$. Generally, the solid angle varies with the magnetar. According to the analysis of Yadigaroglu & Romani (1995), the variation of solid angle for pulsars can be up to 1 order of magnitude. Furthermore, our results from fitting the energy spectra of the known gamma-ray pulsars (Cheng & Zhang 1998) indicate that the solid angle can be from ~ 0.5 to 2.5. Therefore, we believe that the solid angle for magnetars may vary from ~ 0.3 to ~ 3.0.

Now we describe our results for each possible gamma-ray pulsar in detail as follows.

1. 4U 0142+615 (AXP 0142+615) is an AXP with $P = 8.69$ s and $\dot{P} \sim 0.2 \times 10^{-11}$ s s^{-1}. Its X-ray spectrum in the energy range from 2 to 10 keV observed by *ASCA* is well described by a blackbody with effective temperature 0.386 ± 0.005 keV plus a power law with photon index 3.67 ± 0.09 and an absorption column $N_{\mathrm{H}} = (9.5 \times 0.1) \times 10^{21}$ cm^{-2} (White et al. 1996). 4U 0142+615 has no associated supernova remnant and its spin-down timescale is $P/2\dot{P} \sim 10^5$ yr (Wilson et al. 1999), so it may be relatively old. Although it was claimed that the optical counterpart had been found, the optical emission is too faint to admit the presence of a large accretion disk and may be consistent with magnetospheric emission from a magnetar (Hulleman, van Kerkwijk, & Kulkarni 2000a). The distance to this pulsar is not well determined. Liu et al. used $d = 1.5$ kpc. However, Hulleman et al. (2000a) pointed out that the optical extinction A_V to 4U 0142+615 is between to 2.7 and 5.4 mag, as estimated from absorption column density

(White et al. 1996), so this pulsar must be at a distance exceeding about 2.7 kpc. They adopted a distance of 5 kpc. Here we will use two values, 3 and 5 kpc, in our calculation. From equations (2) and (9), we have $f \approx 0.7$ and $L_\gamma \approx 1.7 \times 10^{33}$ ergs s^{-1}. The gamma rays from the outer gap are produced mainly through curvature radiation. In Figure 4, we show the integral fluxes of gamma rays from 4U 0142+615 for three different inclination angles of 45°, 60°, and 75°, where the distance to the pulsar is assumed to be 3 kpc. For comparison, we also show the sensitivities of EGRET and the *Gamma-Ray Large-Area Space Telescope* (*GLAST*), where $\Delta\Omega = 1$ sr in our calculation has been used. It can be seen that *GLAST* will detect the gamma-ray emission from this pulsar although EGRET did not. In fact, the integral flux with energy greater than 100 MeV of this pulsar for $\alpha = 60°$ is $F_\gamma(E \geq 100 \text{ MeV}) \approx 2.2 \times 10^{-8} d_{3\text{ kpc}}^{-2}$ cm^{-2} s^{-1}, which is above the sensitivity of *GLAST* ($\sim 2 \times 10^{-9}$ cm^{-2} s^{-1}).

2. 1E 1048.1−5937 (AXP 1048−5937) was discovered by the *Einstein* satellite and found to pulsate at 6.44 s (Seward, Charles, & Smale 1986). Observations by *EXOSAT* and *Ginga* (Corbet & Day 1990) and by *ROSAT* (Mereghetti 1995) showed that its period derivative is $\sim 5 \times 10^{-4}$ s yr^{-1}. However, the analysis of pulse timing of this pulsar by *ASCA* (Corbet & Mihara 1997) and by *RXTE* (Baykal et al. 2000) shows that the spin-down rate of this pulsar changes. Now the accepted period derivative is (1.5–4) $\times 10^{-11}$ s s^{-1} (Liu et al. 2001). The X-ray spectrum of this pulsar in the energy range of 0.5–10 keV measured with *BeppoSAX* can be described by the sum of a power law with photon index 2.5 ± 0.2 and a blackbody with $kT_s = 0.64 \pm 0.01$ keV, and column density of $N_{\rm H} = (0.45 \pm 0.10) \times 10^{22}$ cm^{-2} (Oosterbrock et al. 1998). This pulsar is situated near $\sim 25'$ diameter remnant G278.8-0.5 associated with the Carina Nebula at a distance of $\sim$2.5–2.8 kpc (e.g., Seward & Chlebowski 1982). This distance is quite consistent with the column density given by Oosterbrock et al. (1998). Here we will use this value as the distance of this pulsar. With $P = 6.44$, $B_{14} = 6.3$, and $T_s = 7.4 \times 10^6$ K, the fractional size of the outer gap is $f \approx 0.23$ and the total gamma-ray luminosity is $L_\gamma \approx 1.2 \times 10^{33}$ ergs s^{-1}. The expected gamma-ray integral flux with energy above 100 MeV from AXP 1048−5937 is $2 \times 10^{-8} (d/2.8 \text{ kpc})^{-2}$ cm^{-2} s^{-1} for $\alpha = 60°$, which is above the sensitivity of *GLAST*.

3. RX J170849−4009 is an AXP that was discovered in a Galactic plane survey with *ASCA* (Sugizaki et al. 1997). This pulsar has a period of 11 s and a period derivative of 2×10^{-11} s^{-1} (Israel et al. 1999); the corresponding surface magnetic field is $\approx 9.5 \times 10^{14}$ G. The X-ray spectrum of this pulsar is soft; the 0.8–10 keV spectrum can be described by a combination of a power law with photon index 2.92 ± 0.3 and a blackbody with $kT_s = 0.41 \pm 0.03$ keV, and column density of $N_{\rm H} = (1.42 \pm 0.2) \times 10^{22}$ cm^{-2} (Sugizaki et al. 1997). This pulsar lies $\sim 8'.5$ from the $\sim 10'$ diameter remnant G346.6-02 (Marsden et al. 2001). There is no kinematic distance estimate to the SNR. Marsden et al. adopted a distance of 3–5 kpc because this distance is consistent with the value of column density given by Sugizaki et al. (1997). With known period, surface magnetic field, and surface temperature, the fractional size of the outer gap is $f \approx 0.47$ and the total gamma-ray luminosity is $L_\gamma \approx 2.7 \times 10^{33}$ ergs s^{-1}. In our model, the gamma-ray integral flux with energy above 100 MeV of this pulsar for $\alpha = 60°$ is $3.5 \times 10^{-8} d_{3\text{ kpc}}^{-2}$ cm^{-2} s^{-1}. Even if the distance to this pulsar is 10 kpc (Sugizaki et al. 1997), we have $F_\gamma(\geq 100 \text{ MeV}) \approx 3.2 \times 10^{-9}$ cm^{-2} s^{-1}. Therefore, the high-energy gamma rays from this pulsar should be detected by *GLAST*.

4. 1E 1841−045 was discovered with the *Einstein* satellite (Kriss et al. 1985). It is at the center of the supernova remnant Kes 73 (G27.4+0.0). *ASCA* observation provided the period of 11.8 s and the period derivative of 4×10^{-11} s s^{-1} of this pulsar (Vasisht & Gotthelf 1997). The X-ray spectrum of 1E 1841−045 is very soft; the 1–10 keV spectrum can be characterized by an absorbed power law with photon index of ~ 3.4 and $N_{\rm H} \approx 3.0 \times 10^{22}$ cm^{-2} (Gotthelf & Vasisht 1997; Gotthelf, Vasisht, & Dotani 1999). The thermal X-ray component of this pulsar has a temperature of 0.55 keV (Liu et al. 2001). Because this pulsar is coincident with Kes 73, the distance is estimated to be the same as that of Kes 73, which is 6.0–7.5 kpc (Sanbonmatsu & Helfand 1992). Putting $P = 11.8$ s, $B = 1.4 \times 10^{15}$ G, and $T_s \approx 6.4 \times 10^6$ K into equations (2) and (9), we have $f \approx 0.39$ and $L_\gamma \approx 2.5 \times 10^{33}$ ergs s^{-1}. The gamma-ray integral flux with energy above 100 MeV is $F_\gamma(\geq 100 \text{ MeV}) \approx 8.7 \times 10^{-9} (d/6 \text{ kpc})^{-2}$ cm^{-2} s^{-1}, which is above the sensitivity of *GLAST*.

5. 1E 2259+58.6 (AXP 2259+58.6) is an X-ray pulsar with a period of 6.98 s and a period derivative of 5.5×10^{-13} s s^{-1}. It has a very soft X-ray spectrum, best described by a combination of a power law with photon index 4.0 ± 0.1 and a blackbody with $kT_s = 0.43 \pm 0.02$ keV, absorbed by a column density $N_{\rm H} = (8.5 \pm 0.4) \times 10^{21}$ cm^{-2} (Rho & Petre 1997). No counterpart at the radio band (Coe, Jones, & Lehto 1994) or at the optical and infra-

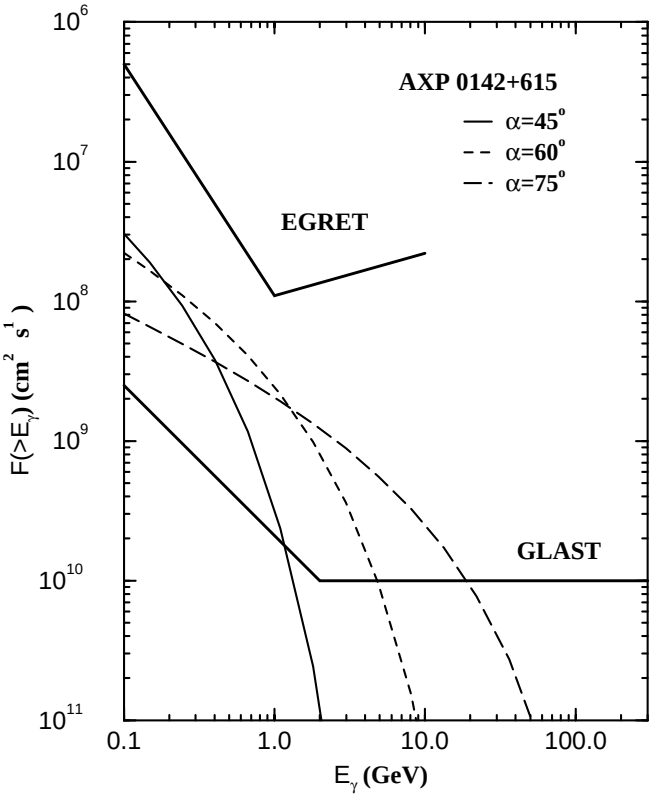

FIG. 4.—Expected integral fluxes of gamma rays from 4U 0142+615 for different inclination angles. For comparison, the sensitivities of EGRET and *GLAST* are shown.

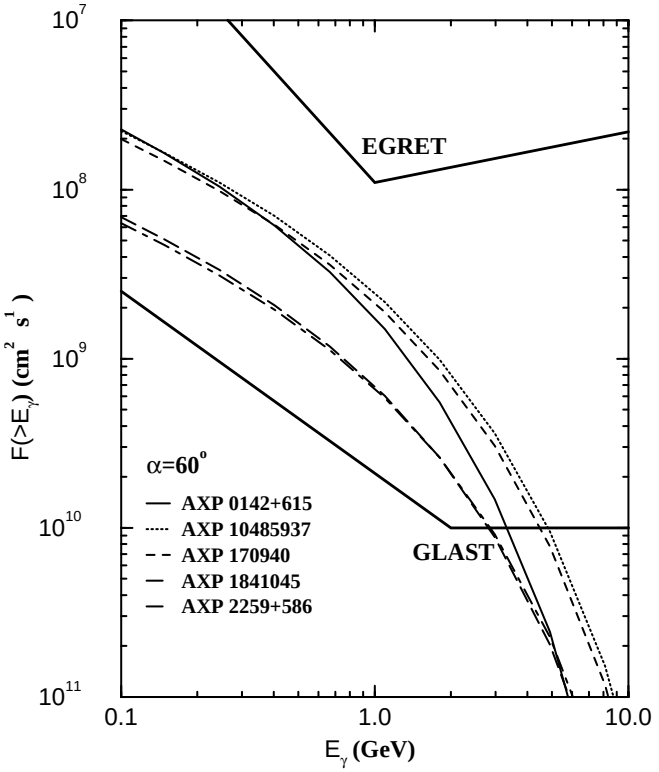

FIG. 5.—Expected integral fluxes of gamma rays from five AXPs with $\alpha = 60°$. The solid line, the dotted line, the short-dashed line, the long-dashed line, and the dot-dashed line are model curves for AXP 0142+615, AXP 1048−5937, AXP 1709−40, AXP 1841−045, and AXP 2259+586, respectively. For comparison, the sensitivities of EGRET and *GLAST* are shown.

red bands (Davies & Coe 1991; Coe & Pightling 1998; Hulleman et al. 2000b) has been found. Because 1E 2259+58.6 is located inside the supernova remnant CTB 109 (G109.1-1.0), the distance to this pulsar is estimated by assuming that the pulsar is the same distance as CTB 109 and that the molecular cloud is either at the same distance or in front. The distance is uncertain; it is in the range 3.5–5.5 kpc (Rho & Petre 1997) or greater than 5 ± 1 kpc (Hulleman et al. 2000b). Here we use the distance of 3.5–5.5 kpc. For the observed period, magnetic field, and temperature of the thermal X-rays, the fractional size of the outer gap is $f \approx 0.76$ and the total gamma-ray luminosity is $L_\gamma \approx 1.1 \times 10^{33}$ ergs s^{-1}. The gamma-ray integral flux with energy above 100 MeV is $F_\gamma(\geq 100 \text{ MeV}) \approx 10^{-8}(d/3.6 \text{ kpc})^{-2}$ cm^{-2} s^{-1} in our model. Therefore, we expect that *GLAST* will detect this AXP.

In Figure 5, we show the gamma-ray integral fluxes of the above five AXPs for $\alpha = 60°$. For comparison, the sensitivities of EGRET and *GLAST* are also shown. Although the gamma-ray integral fluxes of these pulsars are below the sensitivity of EGRET, they are all above *GLAST* sensitivity up to several GeV. Therefore, our predictions can be tested by *GLAST*.

4. DISCUSSION

We have proposed a model to describe high-energy gamma-ray emission from the AXPs. In this model, the high-energy gamma rays are produced inside the outer gap, which is far away from the stellar surface so the local magnetic field is below the quantum critical value. The fractional size of the outer gap depends on the period, surface magnetic field, and surface temperature of the pulsar if the stellar radius is typically ∼15 km for a 1.4 $M_\odot$ neutron star according to the moderate stiff equation of state (Wiringa, Fiks, & Fabrocini 1988). The total gamma-ray luminosity is $\sim 10^{33}$ ergs s^{-1} for the typical parameters of the AXPs, which is about 10^{-2}–10^{-3} of the observed X-ray luminosity. In this model, with known parameters of a pulsar, the high-energy gamma-ray spectrum can be calculated for a given inclination angle. We have calculated the differential fluxes of gamma rays using the typical values of the AXPs (see Figs. 1, 2, and 3). Furthermore, we have applied this model to the AXPs with known periods and period derivatives. All AXPs except for RX J0720.4−3125 have $f \leq 1$, which means that their outer gaps exist. We have calculated the high-energy gamma-ray integral fluxes of five AXPs (see Figs. 4 and 5) and expected that they should be detected by *GLAST*.

In our model, the radius of the neutron star is assumed to be 15 km. From equation (2), the fractional size of the outer gap is proportional to $R^{-3/2}$, i.e., $f \propto R^{-3/2}$. If R changes from 15 to 10 km, then f would change by a factor of 2.25. From equation (9), the total gamma-ray luminosity is proportional to $R^{1.5}$ because $L_\gamma \propto f^3 R^6 \propto R^{-9/2} R^6 \propto R^{3/2}$, so L_γ will decrease by only a factor of ∼1.8 if R is 10 km instead of 15 km. Therefore, the radius of the neutron star has a small effect on the total gamma-ray luminosity in our model. It should be noted that Perna et al. (2001) have fitted X-ray spectra of the known AXPs and SGRs with a model in which the X-ray flux is produced by the thermal emission from a highly magnetized neutron star with an atmosphere made of light elements. Their results indicate that the radii of the AXPs are around 15 km. For example, the radii of 1E 1848.1−5937, 1E 1845−0258, and 4U 0142+61 are about 15.2, 18.0, and 16.1 km, respectively. Therefore, the value of the neutron star that we used is reasonable.

Furthermore, our model depends on the surface temperature of the AXP. The fractional size of the outer gap is proportional to $T_s^{-2/3}$, and the total gamma-ray luminosity is proportional to T_s^{-2}. Generally, the surface temperature of the AXP is estimated from the observed X-ray flux, and it ranges from ∼0.4 to 0.6 keV except for RX J0720.4−3125 (see Table 1). The changes in the fractional size of the outer gap and total gamma-ray luminosity are $f(T_s = 0.4 \text{ keV})/f(T_s = 0.6 \text{ keV}) \approx 1.3$ and $L_\gamma(T_s = 0.4 \text{ keV})/L_\gamma(T_s = 0.6 \text{ keV}) \approx 2.25$, respectively. Such a change has a small effect on the total gamma-ray luminosity in our model.

In our calculations of the high-energy gamma-ray fluxes, a key parameter is the distance to the AXP. Up to now, the distances to the AXPs are uncertain. Therefore, the gamma-ray flux will change by a factor of ∼10 if the distance changes a factor of ∼3. In our calculations, we have used the possible distances for AXP 1841−045, AXP 2259+58.6, AXP 1709−40, and AXP 1048−5937 given by Marsden et al. (2001). For 4U 0142+615, we used $d \geq 2.7$ kpc as a lower limit and assumed $d = 3$ kpc in our calculation. Some of these distances used here are different from those used previously. For example, Liu et al. (2001) listed that the distance to RX 170849−4009 is 10 kpc, while we used the distance 3.5–5 kpc. If we set $d = 10$ kpc, we have $F_\gamma(\geq 100 \text{ MeV}) \sim 3 \times 10^{-9}$ cm^{-2} s^{-1} for $\alpha = 60°$, which is above the sensitivity of *GLAST*. However, if the distance to

1E 1048.1−5937 is 10.6 kpc (Liu et al. 2001), then we have $F_\gamma(\geq 100\ \mathrm{MeV}) \sim 1.4 \times 10^{-9}\ \mathrm{cm}^{-2}\ \mathrm{s}^{-1}$ for $\alpha = 60°$, which is just below the sensitivity of *GLAST*. On the other hand, we have assumed that the beaming solid angle is 1 sr in our calculations; in fact, it should be changed for different pulsars.

The magnetic inclination angle has some effect on the high-energy gamma-ray spectrum in our model. In principle, the increase in the inclination angle results in the shift of the spectrum toward higher energy (see Fig. 1 for differential flux and Fig. 4 for integral flux). As an example, we consider the integral flux of 4U 0142+615: the integral fluxes with energy greater than 100 MeV for $\alpha = 45°$, 60°, and 75° are $3.0 \times 10^{-8} d_{3\ \mathrm{kpc}}^{-2}$, $2.2 \times 10^{-8} d_{3\ \mathrm{kpc}}^{-2}$, and $8.1 \times 10^{-9} d_{3\ \mathrm{kpc}}^{-2}\ \mathrm{cm}^{-2}\ \mathrm{s}^{-1}$, respectively.

Finally, we would like to discuss the relation between gamma-ray luminosity and the spin-down power. Assuming a constant solid angle of photon beaming (say $\Delta\Omega = 1$ sr), Thompson et al. (1999) estimated the high-energy luminosities with photon energies above 1 eV of the known gamma-ray pulsars. They found the following relationship for the known gamma-ray pulsars:

$$L_{\mathrm{HE}} \approx c_1 \dot{N}_{\mathrm{GJ}} \propto L_{\mathrm{sd}}^{1/2} \propto BP^{-2}\ , \qquad (13)$$

where $c_1 \sim 15.2$ ergs, $\dot{N}_{\mathrm{GJ}} \approx 1.7 \times 10^{38} \dot{P}^{1/2} P^{-3/2}\ \mathrm{s}^{-1}$ is the Goldreich-Julian current, and L_{sd} is the spin-down luminosity. Theoretically, both polar cap models and outer gap models give different luminosity dependences compared to this observed luminosity dependence (for a review, see Harding 2001). In fact, the outer gap models predict that the different gamma-ray pulsars have different solid angles of the photon beaming (Romani & Yadigaroglu 1995; Romani 1996; Zhang & Cheng 1997; Cheng, Ruderman, & Zhang 2000; Zhang, Zhang, & Cheng 2000). We have compared the model gamma-ray luminosities with the observed values from known gamma-ray pulsars and shown that they are consistent with each other (Zhang & Cheng 1998). However, according to the model presented here, the expected high-energy luminosity is proportional to $(B/P)^{0.5} T_s^{-2}$ (see eq. [9]), which depends on surface temperature as well. This is because the outer gaps in AXPs do not exist without these stellar X-rays. In other words, the high-energy luminosity is the function of the surface temperature T_s, the period P, and the magnetic field B. We have estimated that the gamma-ray luminosities of five AXPs are $\sim$(1.0–2.7) $\times 10^{33}$ ergs s^{-1}. Applying equation (13) to these AXPs, we find that the high-energy luminosities are ($\sim$1–4) $\times 10^{32}$ ergs s^{-1}. The gamma-ray luminosities predicted by our model are larger than those given by equation (13) by a factor of $\sim$2–12. For example, $L_\gamma/L_{\mathrm{HE}} \sim 2$ for AXP 1048−59 and $L_\gamma/L_{\mathrm{HE}} \sim 12$ for AXP 0142+615. In this sense, our model predicts that more AXPs can be detected by *GLAST* than those predicted by using equation (13) if a constant solid angle of the photon beaming is assumed.

This work is partially supported by an RGC grant of the Hong Kong government and the National Nature Scientific Foundation of China (10073008).

REFERENCES

Baykal, A., Strohmayer, T., Swank, J., Ali Alpar, M., & Stark, M. J. 2000, MNRAS, 319, 205
Cheng, K. S., & Ding, K. Y. 1994, ApJ, 431, 724
Cheng, K. S., Ho, C., & Ruderman, M. 1986, ApJ, 300, 500
Cheng, K. S., Ruderman, M., & Zhang, L. 2000, ApJ, 537, 964
Cheng, K. S., & Zhang, L. 1998, ApJ, 498, 327
Coe, M. J., Jones, L. R., & Lehto, H. 1994, MNRAS, 270, 178
Coe, M. J., & Pightling, S. L. 1998, MNRAS, 299, 223
Corbet, R. H. D., & Day, C. S. R. 1990, MNRAS, 243, 553
Corbet, R. H. D., & Mihara, T. 1997, ApJ, 475, L127
Davies, S. R., & Coe, M. J. 1991, MNRAS, 249, 313
Gotthelf, E. V., & Vasisht, G. 1997, ApJ, 486, L133
Gotthelf, E. V., Vasisht, G., & Dotani, T. 1999, ApJ, 522, L49
Halpern, J. P., & Ruderman, M. 1993, ApJ, 415, 286
Harding, A. K. 2001, in AIP Conf. Proc. 558, High-Energy Gamma-Ray Astronomy, ed. F. A. Aharonian & H. Volk (New York: AIP), (astro-ph/0012268)
Heyl, J. S., & Hernquist, L. E. 1997, ApJ, 491, L95
Heyl, J. S., & Kulkarni, S. R. 1998, ApJ, 506, L61
Hulleman, F., van Kerkwijk, M. H., & Kulkarni, S. R. 2000a, Nature, 408, 689
Hulleman, F., van Kerkwijk, M. H., Verbunt, F. W. M., & Kulkarni, S. R. 2000b, A&A, 358, 605
Hurley, K., et al. 1999, ApJ, 510, L111
Israel, G. L., Covino, S., Stella, L., Campana, S., Haberl, F., & Mereghetti, S. 1999, ApJ, 518, L107
Kouveliotou, C., et al. 1998, Nature, 393, 235
———. 1999, ApJ, 510, L115
Kriss, G. A., Becker, R. H., Helfand, D. J., & Canizares, C. R. 1985, ApJ, 288, 703
Liu, Q. Z., van Paradijs, J., & van den Heuvel, E. P. J. 2001, A&A, 368, 1021
Marsden, D., Lingenfelter, R. E., Rothschild, R. E., & Higdon, J. C. 2001, ApJ, 550, 397
Mereghetti, S. 1995, ApJ, 455, 598
Mereghetti, S. 1999, preprint (astro-ph/9911252)
Mereghetti, S., & Stella, L. 1995, ApJ, 442, L17
Oosterbrock, T., Parmar, A. N., Mereghetti, S., & Israel, G. L. 1998, A&A, 334, 925
Özel, F. 2001, ApJ, submitted (astro-ph/0103277)
Özel, F., Psaltis, D., & Kaspi, V. M. 2001, ApJ, in press (astro-ph/0105372)
Perna, R., Heyl, J., Hernquist, L., Juett, A., & Chakrabarty, D. 2001, ApJ, 557, 18
Rho, J., & Petre, R. 1997, ApJ, 484, 828
Romani, R. W. 1996, ApJ, 470, 469
Romani, R. W., & Yadigaroglu, I.-A. 1995, ApJ, 438, 314
Ruderman, M., & Cheng, K. S. 1988, ApJ, 335, 306
Sanbonmatsu, K. Y., & Helfand, D. J. 1992, AJ, 104, 2189
Seward, F., Charles, P. A., & Smale, A. P. 1986, ApJ, 305, 814
Seward, F. D., & Chlebowski, T. 1982, ApJ, 256, 530
Sugizaki, M., Nagase, F., Torii, K., Kinugasa, K., Asanuma, T., Matsuzaki, K., Koyama, K., & Yamauchi, S. 1997, PASJ, 49, L25
Thompson, C., & Duncan, R. C. 1993, ApJ, 408, 194
———. 1996, ApJ, 473, 322
Thompson, D. J., et al. 1999, ApJ, 516, 297
van Paradijs, J., Taam, R. E., & van den Heuvel, E. P. J. 1995, A&A, 299, L41
Vasisht, G., & Gotthelf, E. V. 1997, ApJ, 486, L129
Wang, F. Y.-H., Ruderman, M., Halpern, J. P., & Zhu, T. 1998, ApJ, 498, 373
White, N. E., Angelini, L., Ebisawa, K., Tanaka, Y., & Ghosh, P. 1996, ApJ, 463, L83
Wilson, C. A., Dieters, S., Finger, M. H., Scott, D. M., & van Paradijs, J. 1999, ApJ, 513, 464
Wiringa, R. B., Fiks, V., & Fabrocini, A. 1988, Phys. Rev. C, 38, 1010
Yadigaroglu, I.-A., & Romani, R. W. 1995, ApJ, 449, 211
Zhang, L., & Cheng, K. S. 1997, ApJ, 487, 370
———. 1998, MNRAS, 294, 177
Zhang, L., Zhang, Y. J., & Cheng, K. S. 2000, A&A, 357, 957